OXIDATION IN ENVIRONMENTS WITH ELEVATED CO_2 LEVELS

Gordon R. Holcomb

National Energy Technology Laboratory
1450 Queen Ave SW, Albany, OR 97321

ABSTRACT

Efforts to reduce greenhouse gas emissions from fossil energy power productions focus primarily on either pre- or post-combustion removal of CO_2. The research presented here examines corrosion and oxidation issues associated with two types of post-combustion CO_2 removal processes—oxyfuel combustion in refit boilers and oxyfuel turbines.

INTRODUCTION

Research in oxyfuel combustion in refit boilers is part of the Office of Research and Development (ORD) project "Materials Performance in Oxyfuel Combustion Environments" and the associated Institute for Advanced Energy Research (IAES) projects at the University of Pittsburgh and Gerald Meier: "Effects of Water Vapor/Carbon Dioxide Mixtures on Alloy Degradation in Environments Relevant to Oxy-Fuel Combustion Systems" and "Effects of Surface Deposits on Alloy Degradation in Environments Relevant to Oxy-Fuel Combustion Systems." Boilers to be refitted for oxyfuel combustion require convective and radiant heat conditions close to existing operations, yet firing with O_2 instead of air changes the boiler environment by replacing large amounts of N_2 with CO_2. This changes convective and radiant heating. Most schemes to accommodate these changes in heating behavior involve recirculating a fraction of the CO_2-rich flue gas back into the boiler. If this is done prior with a gas stream after flue gas desulfurization (FGD), then the boiler will operate with much higher sulfur levels than before the refit. If recirculation is done after FGD, then there will be a large efficiency loss—but sulfur levels will be much the same as before the refit, Fig. 1. For recirculation prior to FGD the major corrosion concern revolves around the elevated sulfur (and perhaps chloride) levels. For recirculation after FGD, the major environment change in the gas phase is the replacement of N_2 with CO_2 (there are also expected changes in ash deposits). The research presented here, which focuses on elevated CO_2 levels, is primarily aimed at the case of recirculation after FGD. Results from laboratory studies in Ar-30%CO_2 environments at 650 °C on two important boiler alloys (T91 and T92) show significant differences in oxidation behavior from heat to heat. Also being examined are Fe-Cr alloys with Ti additions. It is thought that internal Ti carbide formation might increase oxidation resistance by diverting Cr loss to carbide formation.

Research in oxyfuel turbines is part of the ORD project "Materials Performance in Oxyfuel Turbine Environments," which is working in conjunction with the "Zero Emissions Coal Syngas Oxygen Turbo Machinery" project. Gas turbines, such as the Siemens SGT-900 (formerly Westinghouse W251), are prime candidates for use in oxy-fuel turbine systems as the intermediate pressure turbine (IPT), operating with an inlet temperature of approximately 1180 °C.[1-2] Conventional steam turbines are proposed for use as the high pressure turbine (HPT) and low pressure turbine (LPT). The materials performance of turbine and combustor alloys need to be examined for use in gas streams with high concentrations of CO_2. A typical gas composition in the IPT is steam with 10% CO_2 and 0.1-0.2% O_2. Experiments are underway on Nickel- and Cobalt-base alloys, with and without coatings, which comprise the SGT-900 turbine in these types of environments.

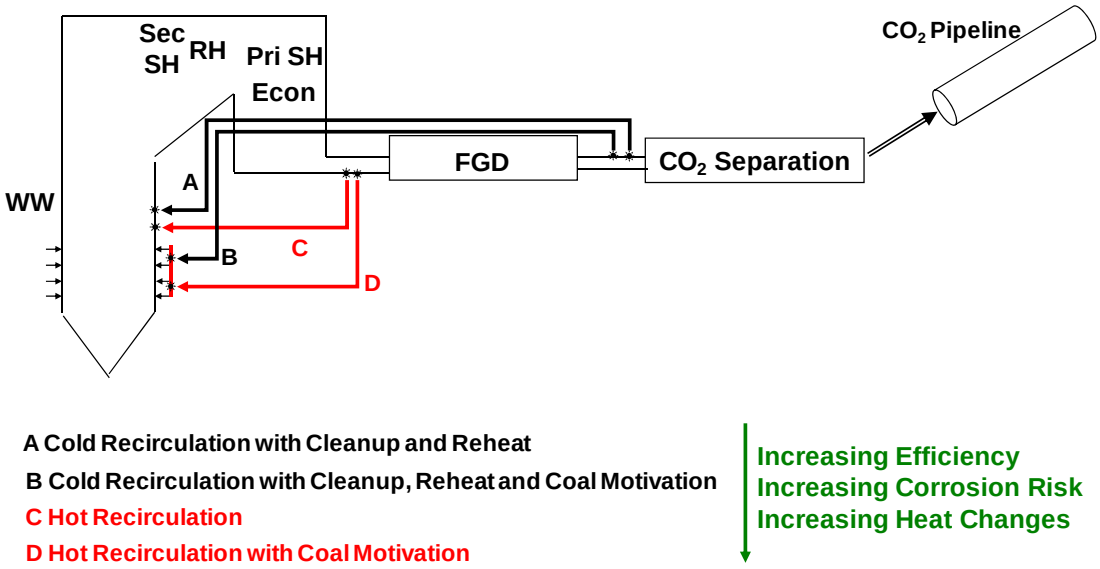

Fig. 1. Oxy-fuel combustion retrofit and possible CO_2 recirculation paths. WW is Waterwall, SH is Superheater, RH is Reheater, Econ is Economizer, and FGD is Flue Gas Desulfurization.

EXPERIMENTAL PROCEDURES

OXY-FUEL BOILERS

Alloys of interest and their compositions are given in Table 1. The tests and results described here are limited to those on the advanced ferritic alloy T92 at a high superheater (SH) temperature of 675 °C. The tests were performed in laboratory tube furnaces with two different gas compositions—one representing air-fired combustion and one representing oxy-fired combustion, Table 2. Table 2 also lists the equilibrium gas composition. In these tests, no attempt was made to provide a catalyst for the sluggish $O_2/SO_2/SO_3$ reactions required to reach equilibrium, so the SO_3 composition in the experiments is likely lower than the equilibrium composition. For each gas composition, the test samples were either bare (without an ash deposit), with ash A (medium sulfur case) or with ash B (high sulfur case), Table 3 and Figs. 2-3. Tests ran for approximately 250 hours.

Table 1. Alloys of interest and composition (wt%) for oxy-fired boiler tests.

Alloy	Fe	Cr	Ni	Mo	C	Mn	Other
T22	Bal	2.07	0.19	0.91	0.102	0.49	
T92	Bal	8.84	0.32	0.32	0.124	0.29	1.83 W
347	Bal	17.2	11.2	0.28	0.061	1.35	
617	2.24	21.6	Bal	7.74	0.102	0.036	10.9 Co

Table2. Gas environments for oxy-fired boiler tests.

Environment	Input					Oxygen-Sulfur Equilibrium		
	N_2	O_2	CO_2	SO_2	H_2O	O_2	SO_2	SO_3
Air-Fired	74.1	6	14.6	0.3	5	5.9	0.16	0.14
Oxy-Fired	0	2.5	60.1	0.9	32.6	2.4	0.61	0.33

Table 3. Ash compositions (wt%) for oxy-fired boiler tests.

Ash	Fe_2O_3	Al_2O_3	SiO_2	Na_2SO_4	K_2SO_4	Calculated Base/Acid
A	31.7	31.7	31.7	2.5	2.5	0.52
B	30.0	30.0	30.0	5.0	5.0	0.54

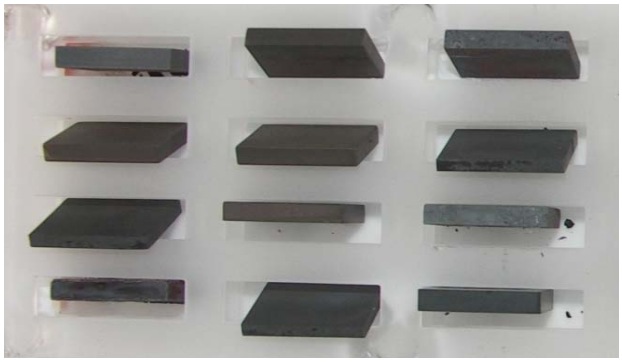

Fig. 2. Bare sample arrangement for oxy-fired boiler tests.

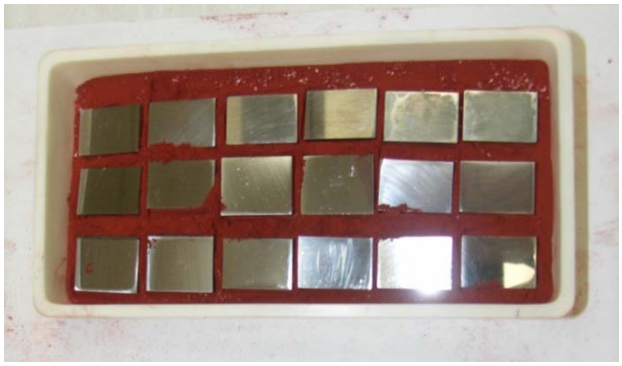

Fig. 3. Ash coated sample arrangement for oxy-fired boiler tests. Shown here prior to the application of the top ash layer.

ARGON-CO_2 TESTS

Tests were also conducted at the University of Pittsburgh on a variety of Fe-Cr alloys for up to 1000 hours in Ar-30% CO_2 environments at 650 °C. Tests were done in tube furnaces and the samples were removed at 100 hour intervals for mass measurements.

OXY-FUEL TURBINES

Nickel-base and cobalt-base alloys that comprise the SGT-900 turbine[2] are shown in Table 4 along with their nominal compositions. A test matrix is shown in Table 5 for 1000 hour exposures in H_2O-10% CO_2-0.2% O_2. Two types of samples were exposed, oxidation coupons (Ox), and low cycle fatigue specimens (LCF). The alloys were either uncoated (Un), had a NiCrAlY bond coat (BC), or had both a BC and a thermal barrier coating (TBC). Only results from uncoated oxidation coupons are presented here.

Table 4. Superalloys tested in the oxy-fired turbine tests. Nominal compositions given in wt%.

Alloy	Ni	Co	Cr	Al	Ti	Mn	Ta+Nb	W	Fe	Mo	C
X-45	10.1	Bal	24.8			0.6		7.8	1.0		0.25
ECY-768	9.7	Bal	23.8	0.1	0.2		3.5	7.0	0.2		0.59
Inconel 738	Bal	8.5	15.8	3.5	3.3		1.7	2.5		1.7	0.12
Inconel 939	Bal	18.9	22.5	1.9	3.8		2.4	2.0			0.14
Udimet 520	Bal	12.5	19.0	2.0	3.0			1.2		6.3	0.06

Table 5. Test matrix for 1000 hour exposures in H_2O-10% CO_2-0.2% O_2

T °C	Type	ECY-768		X-45		IN-738			IN-939		U-520		Total
		Un	TBC	Un	BC	Un	BC	TBC	Un	TBC	Un	BC	
630	LCF										8		8
	Ox	2		2		2			2	1	2	1	12
693	LCF									8			8
	Ox	2	1	2	1	2	1	1	2	1	2	1	16
748	LCF		8		8		7						23
	Ox	2	1	2	1	2	1	1	2	1	2	1	16
821	LCF							8					8
	Ox	2	1	2	1	2	1	1	2		2		14
Spare	Ox	2	1	2	1	2	1	1	2	1	2	1	16
Total	LCF		8		8		7	8		8	8		47
	Ox	10	4	10	4	10	4	4	10	4	10	4	74

RESULTS AND DISCUSSION

OXY-FUEL BOILERS

The T92 samples exposed to the boiler combustion environments experienced extensive corrosion attack. It should be noted that 675 °C is a somewhat higher temperature than expected service temperature for T92. Figures 4-5 show the surface of the bare samples for oxy-fired (Fig. 4) and air-fired (Fig. 5) conditions. Both show indications of extensive scale spallation. Spot analysis showed that the outer scales in both cases, and for all the outer layers shown in Figs. 4-5, were essentially pure iron oxides.

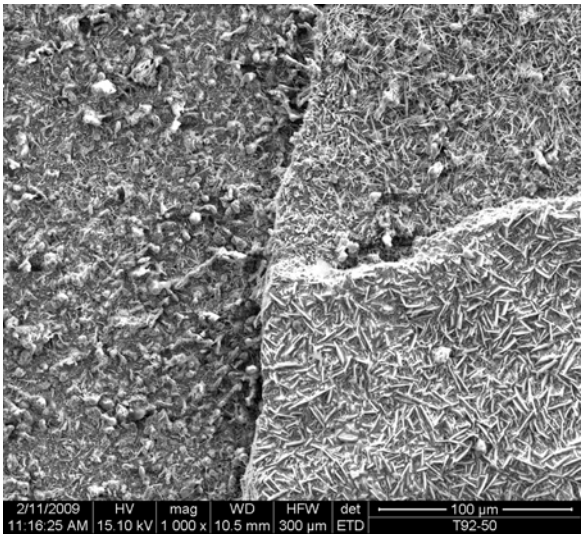

Fig. 4. Surface of bare T92 after exposure at 675 °C for 250 hours in the oxy-fired environment.

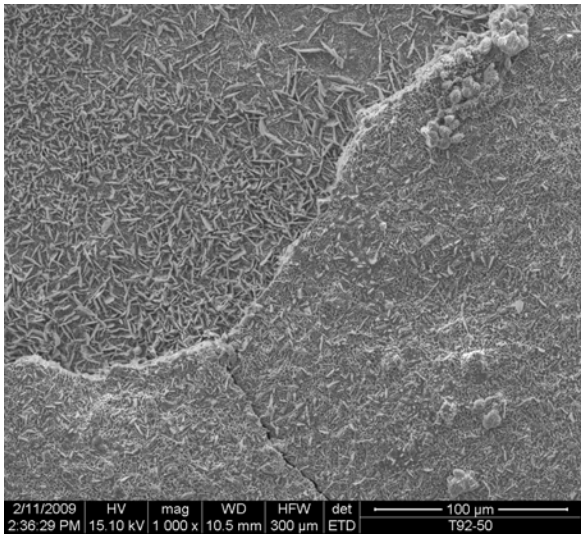

Fig. 5. Surface of bare T92 after exposure at 675 °C for 250 hours in the air-fired environment.

Cross-sections of exposed T92 are shown in Fig. 6 for bare and ash-covered conditions for both oxy-fired and air-fired cases. An outer oxide of essentially pure iron was observed in all cases, with some ash being incorporated into the outer oxide for the ash-covered samples. The inner oxides were striated with high

and low chromium layers. Sulfur was also present in the inner oxide. The sharp division between the inner and outer oxide layers shows the location of the original metal surface.

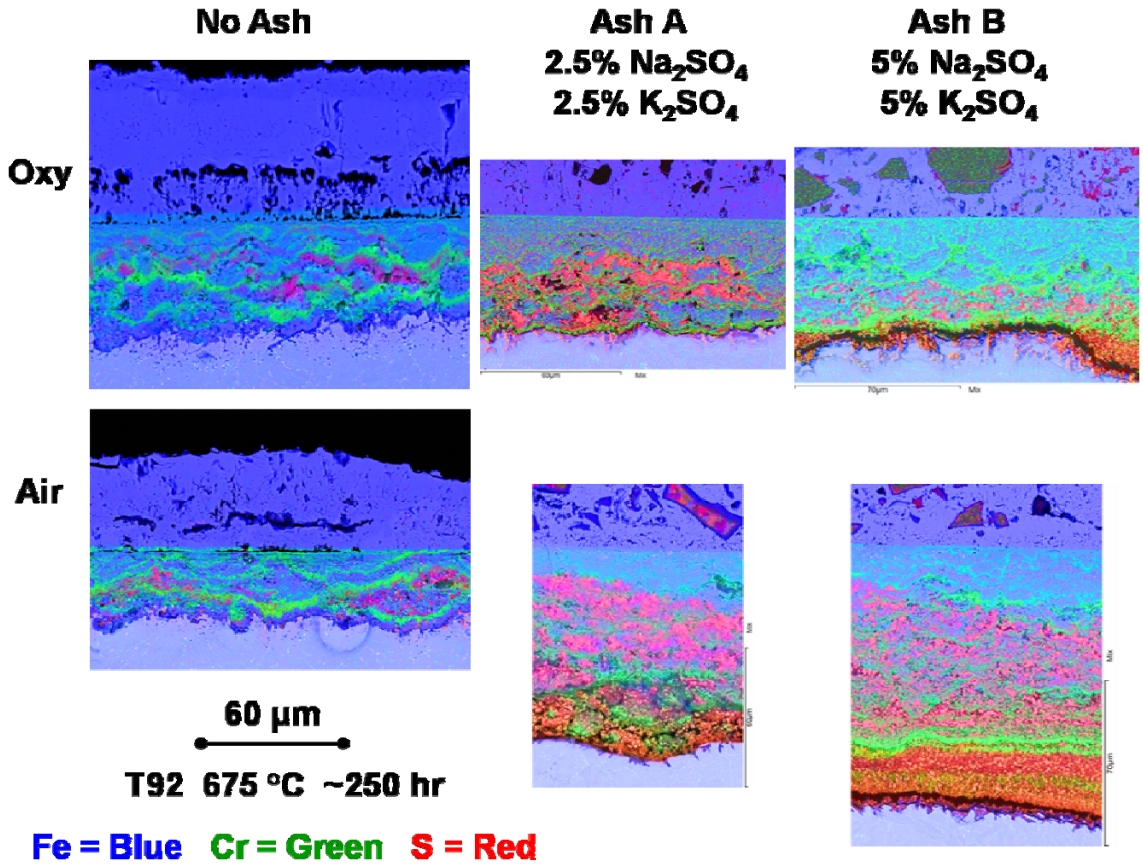

Fig. 6. Cross-sections of bare and ash covered T92 after exposure at 675 °C for 250 hours.

Figure 7 shows that iron and chromium oxides were deposited in the ash. This is indicative of hot corrosion fluxing,[3] where protective oxide scales are dissolved in a molten sulfate phase that develops at the scale-ash interface and precipitate out, with an unprotective morphology, in the ash. "Mud" cracking between the scale and the ash is indicative of a molten phase at temperature. The striations found within the inner oxide may be indicative of cycles in basicity when FeS is formed and then a protective oxide temporarily forms. A similar cycle was seen in nickel under controlled conditions where the basicity was continually measured.[3-4]

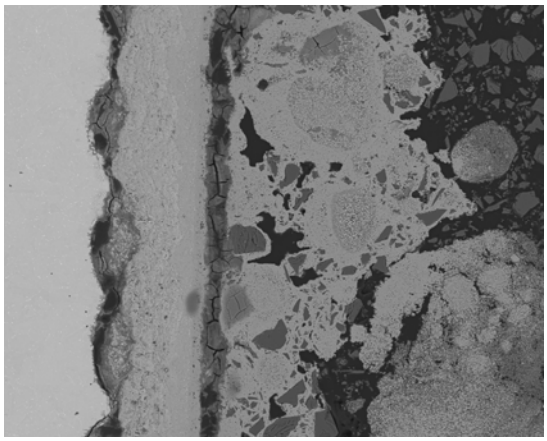

Fig. 7. Low magnification cross-section of T92 after exposure with ash A for 250 hours at 675 °C in the air-fired gas. Metal oxide has precipitated in the ash phase. "Mud" cracking between the scale and the ash is indicative of a molten phase at temperature.

ARGON-CO_2 TESTS

Figure 8 shows results for various Fe-Cr alloys exposed at 650 °C in Ar-CO_2 environments.[5] The surfaces feature protective Cr-rich oxide regions and rapidly oxidizing Fe-oxide regions. The alloys Fe-10Cr and Fe-13Cr exhibited rapid corrosion and a large surface fraction of Fe-oxide. After a short protective time period, T91 also had rapid corrosion. Even with a relatively low amount of Cr (~9 wt%), T92 had very little mass gain and had results similar to the Fe-22Cr alloys.

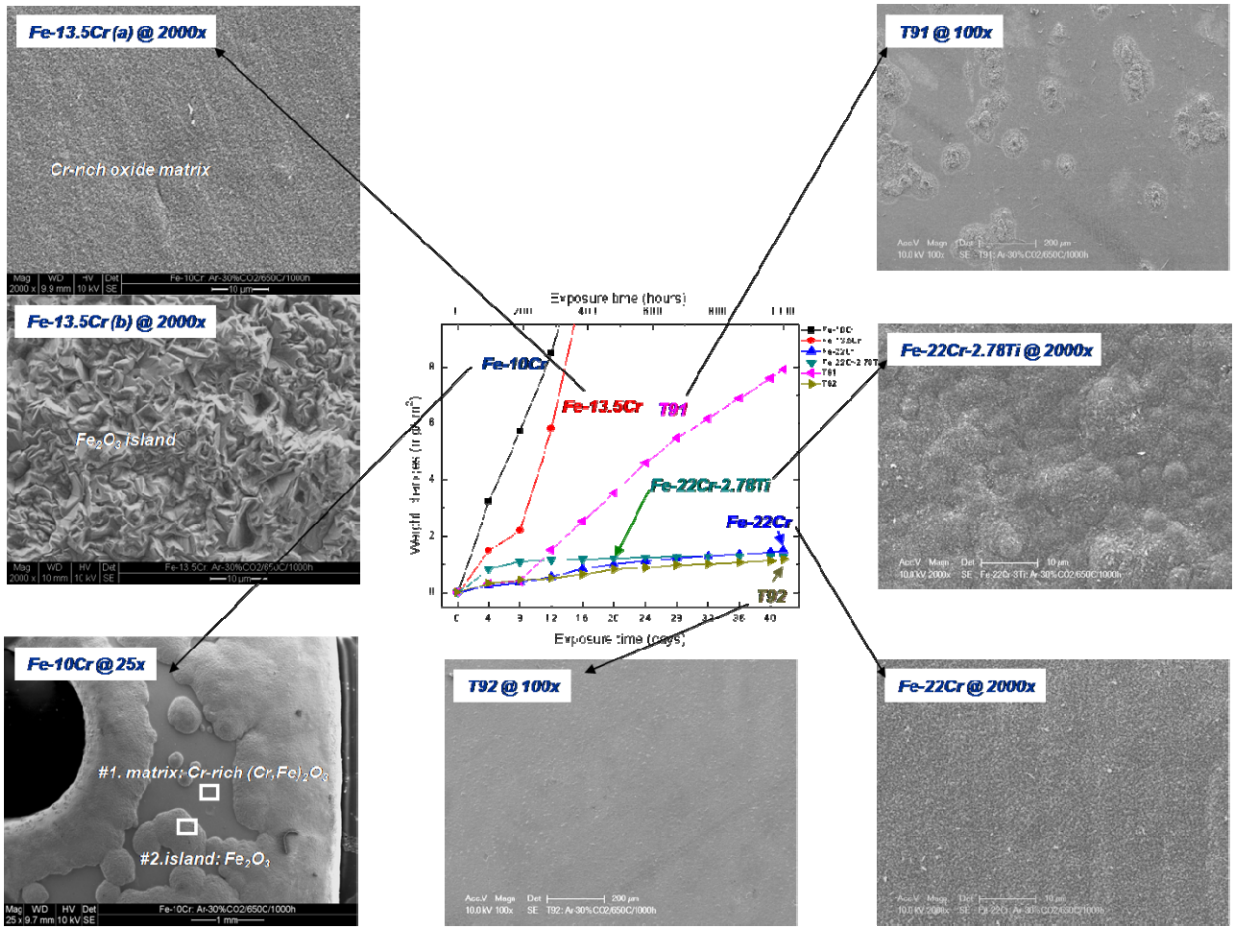

Fig. 8. Results for various Fe-Cr alloys exposed at 650 °C in Ar-CO_2 environments. Surfaces feature protective Cr-rich oxide regions and rapidly oxidizing Fe-oxide regions. Courtesy of Jung, *et al*.[5]

OXY-FUEL TURBINES

Overall mass change results showed that the cobalt-base alloys exhibited less mass gain at 748 °C than the nickel-base alloys. However, the downward trend for some of the cobalt-base alloys after the first 250 hours of exposure could show tendencies towards scale spallation or chromia evaporation. Mass gains for all the alloys were low and very similar to each other at 630 °C. Figures 9-10 show the mass change results for alloys X-45 and Udimet 520.

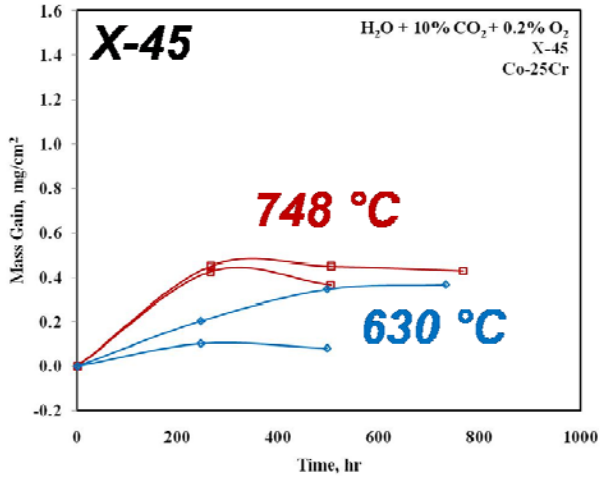

Fig. 9. Mass change for Co-base alloy X-45 after exposure in H_2O-10%CO_2-0.2%O_2.

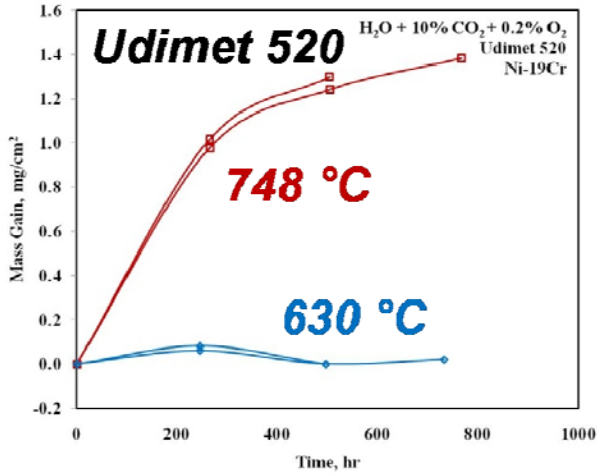

Fig. 10. Mass change for Ni-base alloy Udimet 520 after exposure in H_2O-10%CO_2-0.2%O_2.

THERMODYNAMICS

In environments high in CO_2 and low in O_2, where CO_2 may act as an oxidant, C injection into the alloy may occur. Figures 11-12 show the expected phases, as derived by Thermocalc,[6-7] for Fe-9Cr and Fe-9Cr-2W as a function of C content. The expected carbide phases change with C content.

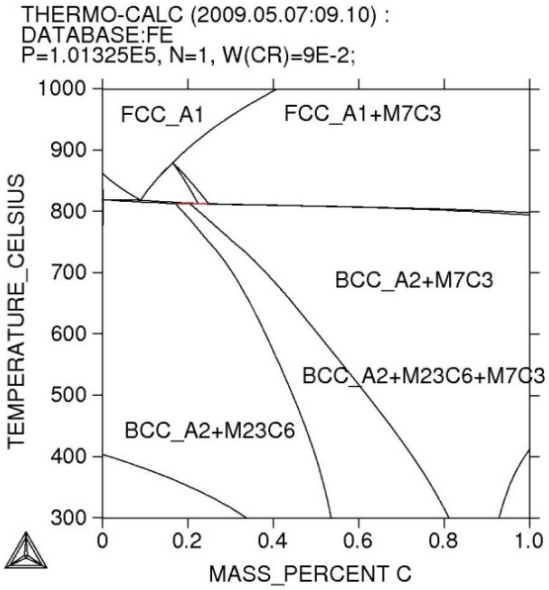

Fig. 11. Fe-9Cr-C isopleth.[6-7]

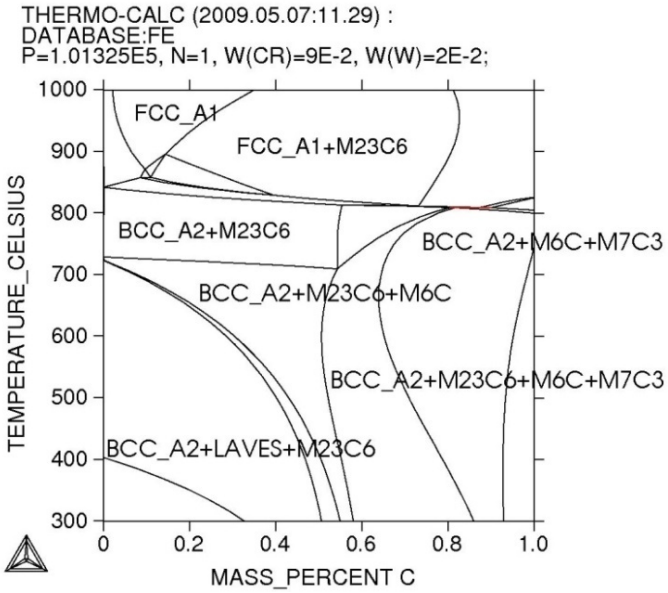

Fig. 12. Fe-9Cr-2W-C isopleth.[6-7]

Since Cr-carbides are more stable than Fe-carbines, it is expected that injected C would tie up Cr that gives these alloys oxidation protection. Figures 13-14 show how the weight fraction of Cr in the BCC phase of the alloy decreases with increasing C content.[6-7]

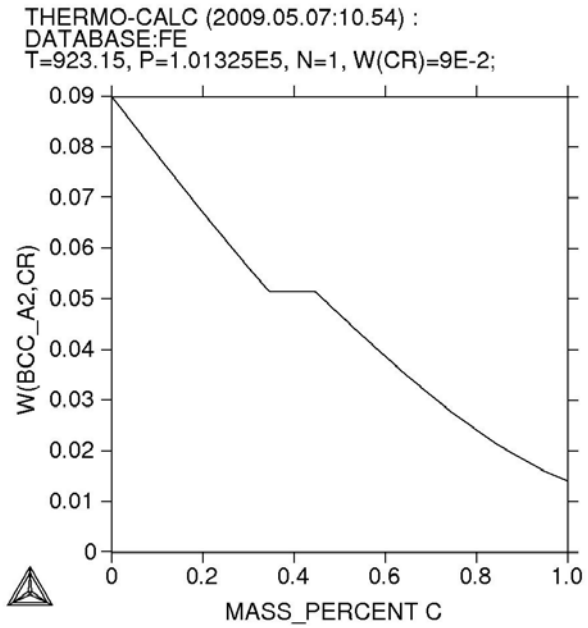

Fig. 13. Mass fraction of Cr in the BCC phase at 650 °C in Fe-9Cr as a function of C content.[6-7]

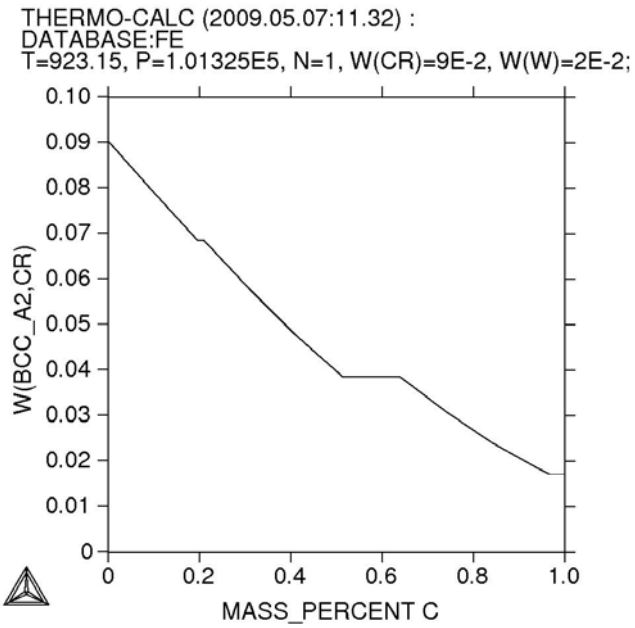

Fig. 14. Mass fraction of Cr in the BCC phase at 650 °C in Fe-9Cr-2W as a function of C content.[6-7]

The addition of minor alloying elements, such as W or Ti, that form more stable carbides than Cr does, have the potential to "buffer" the alloy by the formation of W-carbides or Ti-carbides instead of Cr-carbides, thereby allowing more Cr to remain available for oxidation protection. The calculations shown in Figs. 15-16 attempt to show this type of behavior. In these figures, Fe-9Cr-0.6C and Fe-9C-2W-0.6C are "oxidized" by showing the phase fraction as a function of oxygen. In Fig. 15, the amount of BCC phase linearly decreases with O content. In Fig. 16, the amount of BCC phase shows horizontal regions where Cr-carbides are being preferentially oxidized and leaving W-rich carbides behind.

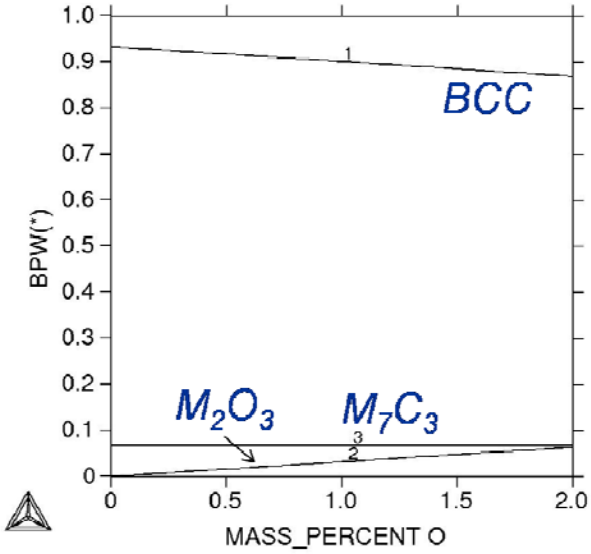

Fig. 15. Phase fraction as a function of oxygen for Fe-9Cr-0.6C at 650 °C.[6-7]

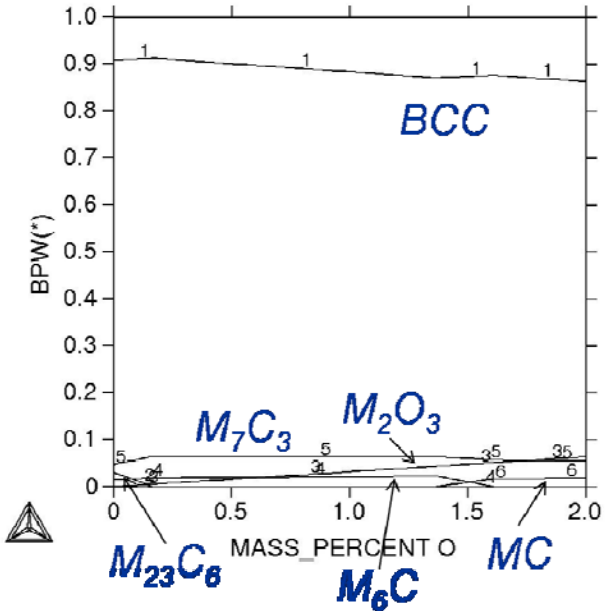

Fig. 16. Phase fraction as a function of oxygen for Fe-9Cr-2W-0.6C at 650 °C.[6-7]

T91 AND T92 IN SEVERAL ENVIRONMENTS WITH ELEVATED CO_2 LEVELS

Figure 17 shows a comparison of the effects from various environments on the oxidation rates of T91 and T92. The lowest rates are for Ar-30%CO_2 (ref 5) and moist air.[8] Above them are slightly higher rates in steam.[9] The highest rates are for exposures to steam + 10%CO_2 + 0.2% O_2 (the conditions of the oxy-fuel turbine tests). These rates are higher than the components of this type of environment would suggest.

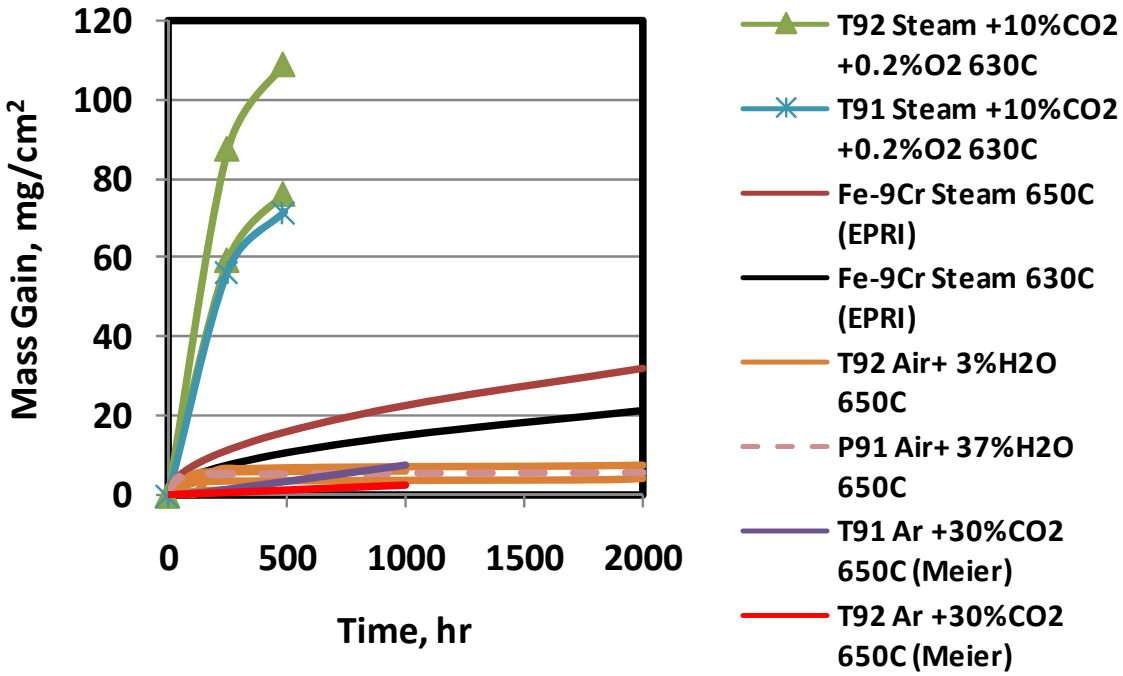

Fig. 17. Oxidation kinetics for T91 and T92 in a variety of environments.[5,8-9]

SUMMARY

Materials performance challenges exist in developing carbon-capture technologies such as oxy-fired boilers and oxy-fired turbines. Elevated CO_2 levels in these systems may result in increased oxidation rates and carburization of the alloys that can deplete Cr available for oxidation protection. Thermodynamics were used to predict phase structures and phase compositions during carburization and subsequent oxidation.

ACKNOWLEDGEMENTS

Funding and support for the research described here were funded through the following projects and contracts:

- Materials Performance in USC Steam, ORD-09-220682-1.
- Materials Performance in Oxyfuel Combustion Environments, ORD-09-220683.
- Materials Performance in Oxy-fuel Turbine Environments, ORD-09-220682-2/a.

- Gerald Meier, Effects of Water Vapor/Carbon Dioxide Mixtures on Alloy Degradation in Environments Relevant to Oxy-Fuel Combustion Systems, DE-AC26-04NT41817, IAES 1.1.3.
- Gerald Meier, Effects of Surface Deposits on Alloy Degradation in Environments Relevant to Oxy-Fuel Combustion Systems, DE-AC26-04NT41817, IAES 1.1.8.

REFERENCES

1. R. E. Anderson, S. MacAdam, F. Viteri, D. O. Davies, J. P. Downs, and A. Paliszewski, "Adapting Gas Turbines to Zero Emission Oxy-Fuel Power Plants," Proceedings of ASME Turbo Expo 2008: Power for Land, Sea and Air, GT 2008-51377, Berlin, Germany, June 9-13, 2008.
2. R. E. Anderson, F. Viteri, R. Hollis, M. Hebbar, J. Downs, D. Davies, and M. Harris, "Application of Existing Turbomachinery for Zero Emissions Oxy-Fuel Power Systems," Proceedings of ASME Turbo Expo 2009: Power for Land, Sea and Air, GT 2009-59995, Orlando, FL, June 8-12, 2009.
3. R. A. Rapp, Corrosion Science, 44 (2002), 209-221.
4. N. Otsuka and R. A. Rapp, J. Electrochem. Soc., 137 (1990) 46.
5. K. Jung, N. Mu, F. S. Petit, and G. H. Meier, "Effects of Oxyfuel Atmospheres and Surface Deposits on Alloy Corrosion," poster at the 23rd Annual Conference on Fossil Energy Materials, Pittsburgh, PA, May 12-14, 2009, U.S. Department of Energy, Office of Fossil Energy, Advanced Research Materials (2007).
6. Thermo-Calc, Diffusion Simulation Software, Version S, Thermo-Calc Software AB, Stockholm, Sweden (2008).
7. N. Saunders, Fe-*DATA*, Version 6, Thermotech Ltd, Surrey Technology Centre, Surrey, UK (2000).
8. G. R. Holcomb, D. E. Alman, Ő. N. Doğan, J. C. Rawers, K. K. Schrems, and M. Ziomek-Moroz, "Steam Turbine Materials and Corrosion," in *Proceedings of the 21st Annual Conference on Fossil Energy Materials*, Knoxville, TN, April 30-May 1, 2007, U.S. Department of Energy, Office of Fossil Energy, Advanced Research Materials (2007).
9. A. I. G. Wright and P. F. Tortorelli, "Program on Technology Innovation: Oxide Growth and Exfoliation on Alloys Exposed to Steam," EPRI, Palo Alto, CA: 2007. 1013666.